

R-mode oscillations of differentially and rapidly rotating Newtonian polytropic stars

Shigeyuki Karino¹*, Shin'ichirou Yoshida², Yoshiharu Eriguchi¹

¹ Department of Earth Science and Astronomy,
Graduate School of Arts and Sciences,

University of Tokyo, Komaba, Meguro, Tokyo 153-8902, Japan

² SISSA, Via Beirut 2-4, 34013 Trieste, Italy

November 5, 2018

Abstract

For the analysis of the r-mode oscillation of hot young neutron stars, it is necessary to consider the effect of *differential rotation*, because viscosity is not strong enough for differentially rotating young neutron stars to be lead to uniformly rotating configurations on a very short time scale after their birth. In this paper, we have developed a numerical scheme to solve r-mode oscillations of differentially rotating polytropic inviscid stars. This is the extended version of the method which was applied to compute r-mode oscillations of uniformly rotating Newtonian polytropic stars. By using this new method, we have succeeded in obtaining eigenvalues and eigenfunctions of r-mode oscillations of differentially rotating polytropic stars.

Our numerical results show that as the degree of differential rotation is increased, it becomes more difficult to solve r-mode oscillations for slightly deformed configurations from sphere compared to solving r-mode oscillations of considerably deformed stars. One reason for it seems that for slightly deformed stars corotation points appear near the surface region if the degree of differential rotation is strong enough. This is similar to the situation that the perturbational approach of r-mode oscillations for *slowly rotating* stars in *general relativity* results in a singular eigenvalue problem.

1 Introduction

Recent intensive as well as extensive investigations of the r-mode instability have revealed its important role in neutron star physics ([1, 2]; for a review see e.g. [3, 4]; for r-mode oscillations see [5, 6, 7]). At the early stage of those investigations, the r-mode oscillations were found to become significantly unstable for some range of the core temperature [8, 9, 10]. However, models used in those papers were too simplified to deduce a decisive conclusion for real neutron stars because one could only obtain r-mode oscillations of *uniformly* and *slowly* rotating Newtonian polytropic stars and apply the results to realistic neutron stars.

Actual neutron stars are more complicated configurations. There are many factors to be included to get a definite answer about the effect of the r-mode instability on them. For example, neutron stars are general relativistic objects, they are generally expected to be rapidly rotating at their birth, the physical states of the interior

*E-mail: karino@valis.c.u-tokyo.ac.jp

cannot be quantitatively approximated by polytropic relations, the surface of the neutron stars is not considered to be fluid, they have magnetic fields and so on.

The rotation law is one of such factors. Although in almost all papers about the r-mode instabilities neutron stars are assumed to rotate uniformly, newly born neutron stars whose ages are less than 1 year should be considered to be rotating differentially. Some neutron stars are newly formed from core collapses of massive stars on a dynamical time scale without enough time to redistribute the angular momentum due to viscosity and rotate differentially. (At some stages of recycled neutron stars, they may begin to rotate differentially due to instability of f-mode oscillations via gravitational wave emission because angular momentum increase due to accretion onto old neutron stars leads them to bifurcation points to configurations within which there exists internal motion. However, this instability results in non-axisymmetric configurations and they are out of the scope of the present paper.) Thus we need to study the effect of differential rotation of newly born neutron stars on the r-mode oscillations.

Moreover, some authors discuss the onset of differential rotation of a star due to self-induction by r-mode oscillations. Spruit [11] argued that the back-reaction of gravitational radiation by the r-mode oscillation on the stellar fluid may induce the differential rotation of the star. Rezzolla et al. [12, 13, 14] studied a drift induced by the r-mode oscillation of the stellar fluid which is initially uniformly rotating, and concluded that the r-mode instability may lead to the differential rotation of the star. By using numerical simulation of stellar hydrodynamics, Lindblom et al. [15] studied non-linear evolution of an initially uniformly rotating star by the r-mode instability and found that the stellar fluid develops strong differential rotation. Thus in the general context of the r-mode instability, it seems to be important to investigate the r-mode oscillations of differentially rotating stars.

In our present investigation, by extending the numerical method which we developed to compute r-mode oscillations of uniformly and rapidly rotating polytropes [16, 17], we have succeeded in obtaining sequences of r-mode oscillations for differentially rotating polytropic stars (in a different context, the r-mode oscillations of configurations with *slightly* differential rotation are treated in [18, 19]). From our numerical results for differentially rotating stars, we have found that, if the degree of differential rotation is small, r-mode oscillations of the ordinary type can be obtained. Here r-modes of the ordinary type mean that the eigenfrequency has discrete spectrum. However, when the degree of differential rotation becomes sufficiently large, no r-mode oscillations of the ordinary type seem to be allowed, because in the surface region of the star corotation points appear and the basic equation becomes singular there.

Since the purpose of this paper is to show the characteristic feature of the r-mode oscillation of differentially rotating stars, we only present a limited results of numerical computations, i.e. for the $m = 2$ mode, where m is the azimuthal mode number of the perturbation.

2 Formulation of the problem

We study the effect of differential rotation on the r-mode oscillations by solving the linearized equations of fluid motions of stars. The scheme employed in this paper is the extended version of that developed to analyze the r-mode oscillation of uniformly rotating Newtonian polytropes [16, 17]. Therefore, we will explain the scheme only briefly.

2.1 Assumptions on unperturbed stars

We construct axisymmetric equilibrium configurations of differentially rotating polytropic inviscid stars in Newtonian gravity by employing the Straight-Forward-Newton-Raphson method [20]. Here the polytropic relation is expressed by the following formula:

$$p = K\rho^{1+\frac{1}{N}}, \quad (1)$$

where p , ρ , K and N are the pressure, the density, the polytropic constant and the polytropic index, respectively. In this paper polytropes with $N = 0.5, 1.0$ and 1.5 are investigated.

As for the rotation law of differentially rotating unperturbed stars, two kinds of angular velocity, Ω , distribution are employed:

$$\Omega = \frac{\Omega_c A^2}{(R/R_{\text{eq}})^2 + A^2}, \quad (2)$$

and

$$\Omega = \frac{\Omega_c A}{\sqrt{(R/R_{\text{eq}})^2 + A^2}}. \quad (3)$$

where R is the distance from the rotation axis, R_{eq} is the equatorial radius of the star and Ω_c is the central angular velocity. The quantity A is a parameter which represents the degree of differential rotation. The rotation becomes more differential as A becomes smaller. On the other hand, when we consider the limit of $A \rightarrow \infty$, the stellar rotation tends to uniform rotation in both cases. For the region where $R/R_{\text{eq}} \gg A$, the former law, Eq. (2), tends to that of constant specific angular momentum distribution, while the latter, Eq. (3), tends to that of constant linear velocity distribution. Thus we will call the former as a j-constant rotation law and the latter as a v-constant rotation law, hereafter.

2.2 Linearized basic equations for perturbed stars

As mentioned before, the scheme to handle the r-mode oscillation of differentially rotating polytropes is the extended version of that to solve the perturbed fluid equations for uniformly rotating polytropes by the Newton-Raphson iteration scheme [16, 17].

Our basic equations consist of linearized parts of the following equations: 1) the continuity equation, 2) the θ -component of the vorticity conservation equation, or the compatibility equation between the r - and φ -components of the equation of motion, 3) the φ -component of the vorticity conservation equation, or the compatibility equation between the r - and θ -components of the equation of motion, and 4) the φ -component of the equation of motion. The linearized gravitational potential in the integral form is used in the φ -component of the equation of motion. Here, the spherical coordinates (r, θ, φ) are used.

Concerning the perturbed quantities, we assume the harmonic expansion of the physical quantities as

$$\delta f(r, \theta, \varphi, t) = \sum_m \exp(-i\sigma t + im\varphi) f_m(r, \theta), \quad (4)$$

where f denotes a certain physical quantity, δ is the Euler perturbation of the corresponding quantity, σ is the frequency of the oscillation and m is the mode number. Because of the stationary and axisymmetric nature of unperturbed stars the equations are separable with respect to the variables t and φ . Thus our basic equations are characterized by σ and m . The perturbed fluid equations are expressed as follows:

$$\rho_0 \frac{\partial \delta u_r}{\partial r} + \left(\frac{2\rho_0}{r} + \frac{\partial \rho_0}{\partial r} \right) \delta u_r + \frac{\rho_0}{r} \frac{\partial \delta v_\theta}{\partial \theta} + \frac{1}{r} \left(\rho_0 \cot \theta + \frac{\partial \rho_0}{\partial \theta} \right) \delta v_\theta + \frac{m\rho_0}{r \sin \theta} \delta w_\varphi = (\sigma - m\Omega) \delta \rho, \quad (5)$$

$$\begin{aligned} & \frac{r \sin^2 \theta}{m} \left(2\Omega + r \frac{\partial \Omega}{\partial r} \right) \frac{\partial \delta u_r}{\partial r} + \frac{1}{m} \left[m(m\Omega - \sigma) + \sin^2 \theta \left(2\Omega + 4r \frac{\partial \Omega}{\partial r} + r^2 \frac{\partial^2 \Omega}{\partial r^2} \right) \right] \delta u_r \\ & + \frac{r \sin^2 \theta}{m} \left(2\Omega \cot \theta + \frac{\partial \Omega}{\partial \theta} \right) \frac{\partial \delta v_\theta}{\partial r} + \frac{r \sin^2 \theta}{m} \left[2\Omega \cot \theta + \frac{\partial \Omega}{\partial \theta} + 2r \cot \theta \frac{\partial \Omega}{\partial r} + r \frac{\partial^2 \Omega}{\partial r \partial \theta} \right] \delta v_\theta \\ & + \frac{r \sin \theta}{m} (m\Omega - \sigma) \frac{\partial \delta w_\varphi}{\partial r} + \frac{\sin \theta}{m} \left[(m\Omega - \sigma) + 2m\Omega + mr \frac{\partial \Omega}{\partial r} \right] \delta w_\varphi = 0, \quad (6) \end{aligned}$$

$$\begin{aligned} & (\sigma - m\Omega) \frac{\partial \delta u_r}{\partial \theta} - m \frac{\partial \Omega}{\partial \theta} + r(m\Omega - \sigma) \frac{\partial \delta v_\theta}{\partial r} + \left[(m\Omega - \sigma) + mr \frac{\partial \Omega}{\partial r} \right] \delta v_\theta \\ & + 2r \cos \theta \Omega \frac{\partial \delta w_\varphi}{\partial r} - 2 \sin \theta \Omega \frac{\partial \delta w_\varphi}{\partial \theta} + 2 \left(r \cos \theta \frac{\partial \Omega}{\partial r} - \sin \theta \frac{\partial \Omega}{\partial \theta} \right) \delta w_\varphi = 0, \quad (7) \end{aligned}$$

$$\begin{aligned} & K \left(1 + \frac{1}{N} \right) \rho_0^{\frac{1}{N}-1} \frac{m}{r \sin \theta} \delta \rho + \frac{m}{r \sin \theta} \delta \phi + \sin \theta \left(2\Omega + r \frac{\partial \Omega}{\partial r} \right) \delta u_r \\ & + \left(2\Omega \cos \theta + \sin \theta \frac{\partial \Omega}{\partial \theta} \right) \delta v_\theta + (m\Omega - \sigma) \delta w_\varphi = 0. \quad (8) \end{aligned}$$

$$\begin{aligned} \delta \phi = & -4\pi G \sum_{n,m} \int_0^{\frac{\pi}{2}} d\theta' \sin \theta' \frac{(n-m)!}{(n+m)!} P_n^m(\cos \theta) P_n^m(\cos \theta') \\ & \times \int_0^{r_s(\theta')} dr' r'^2 f_n(r, r') \delta \rho \\ & -4\pi G \sum_{n,m} \int_0^{\frac{\pi}{2}} d\theta' \sin \theta' \frac{(n-m)!}{(n+m)!} P_n^m(\cos \theta) P_n^m(\cos \theta') \\ & \times f_n(r, r_s(\theta')) \rho_0(r_s(\theta'), \theta') \delta r_s(\theta'), \quad (9) \end{aligned}$$

where $r_s(\theta)$ is the surface radius of the equilibrium configuration and δr_s is the change of the surface. Here, functions $f_n(r, r')$ are defined as

$$f_n(r, r') = \begin{cases} \frac{1}{r} \left(\frac{r'}{r} \right)^n & (r' < r) \\ \frac{1}{r'} \left(\frac{r}{r'} \right)^n & (r' \geq r), \end{cases} \quad (10)$$

and ρ_0 denotes the mass density of the equilibrium states, whereas δu_r , δv_θ , δw_φ , $\delta \rho$ and $\delta \phi$ are the Euler perturbations of the r -, θ - and φ -components of the velocity in the corresponding orthonormal frame, the density and the gravitational potential, respectively.

In these equations, we have made use of the following adiabatic perturbation between the pressure and the density:

$$\frac{\delta p}{p} = \left(1 + \frac{1}{N} \right) \frac{\delta \rho}{\rho}, \quad (11)$$

where δp is the Euler perturbation of the pressure.

2.3 Boundary conditions

Since we treat infinitesimal oscillations around equilibrium configurations, all the perturbed quantities must behave regularly throughout the whole space. In particular, the Eulerian change of the density and the Eulerian change of the gravitational potential must be regular functions of the position.

As for the perturbed flow velocity, the boundary condition on the surface can be expressed as

$$\frac{\partial \rho_0}{\partial r} \left(\delta u_r - \frac{1}{r_s} \frac{dr_s}{d\theta} \delta v_\theta \right) + (m\Omega - \sigma) \delta \rho = 0. \quad (12)$$

This condition comes from a requirement that the fluid element on the equilibrium surface is displaced to the perturbed surface.

3 Numerical results

We can obtain eigenvalues and eigenfunctions by solving numerically the basic equations mentioned above by the Newton-Raphson iteration scheme, together with the boundary condition. In actual computations, we use 44 mesh points in r -direction and 11 mesh points in θ -direction.

In Figure 1, the eigenvalues of equilibrium sequences with different values of the parameter A are plotted against the ratio of the rotational energy, T , to the absolute value of the gravitational energy, W , for the $m = 2$ mode of $N = 1$ polytropes. In this figure, for the sake of simplicity, the eigenvalues are normalized by using the central angular velocity. This choice of the normalization constant results in decreasing of the eigenfrequencies for the smaller value of A or for the larger degree of differential rotation. It is clearly seen that the eigenvalues decrease as the ratio $T/|W|$ increases for a given value of A . Terminal points of sequences at the larger end of $T/|W|$ correspond to final models beyond which our present code could not give converged solutions.

Figure 2 shows θ -component of the perturbed velocity on the equatorial plane for the $m = 2$ oscillation of $N = 1$ polytropes with different degrees of nonuniform rotation. The horizontal axis is the normalized radius. The equilibrium stars are rotating rather rapidly, i.e. $r_p = 0.7$. Here r_p is the axis ratio which is defined by

$$r_p = r_{\text{ax}}/r_{\text{eq}}, \quad (13)$$

where r_{ax} and r_{eq} are the stellar radius along the rotational axis and that on the equatorial plane, respectively.

Three curves in Figure 2 correspond to equilibrium models of rigid rotation, differential rotation with the parameter $A = 1.3$ and extremely differential rotation with $A = 0.6$, respectively. The values of $T/|W|$ are almost the same for these models, i.e. $T/|W| = 0.073, 0.082$ and 0.080 for the uniformly rotating model, the model with $A = 1.3$ and the model with $A = 0.6$, respectively. Thus we can regard these three models as those with the same rotational amount but different degrees of differential rotation. From this figure, we can see that if we take the differential rotation into consideration, oscillatory motions of the stellar fluid are confined only in the narrow layer near the surface of the star for a model with larger degree of differential rotation. In other words, for differentially rotating models, if the degree of differential rotation is large, only the fluid near the surface region can oscillate appreciably but the inner bulk of the star almost remains at its original position. This behavior can be seen not only in the equatorial plane but also in all θ - directions.

In Figure 3, eigenfrequencies of r-mode oscillations for the $m = 2$ mode of differentially rotating polytropes with several polytropic indices are plotted against

the value of $T/|W|$, i.e. $N = 0.5, 1.0$ and 1.5 . Here we have used the rotation law (2) with $A = 1.3$. Terminal points of these sequences are final models beyond which our code could not give solutions to the linearized basic equations because of very slow convergence. From this figure, it is clear that, although the values of σ/Ω_c are not the same, the tendency of decrease of the normalized eigenfrequency as increase of $T/|W|$ is the same.

For oscillations of differentially rotating stars, we need to pay attention to emergence of corotation points at some places in the stellar interior because appearance of corotation points corresponds to a singular behavior of the basic equations (see e.g. [21]). Here corotation points are defined as points at positions where the following condition is satisfied:

$$\hat{\sigma} \equiv \sigma - m\Omega = 0. \quad (14)$$

The condition of appearance of corotation points can be expressed by a simple inequality for differentially rotating stars. For the j-constant rotation law, Eq. (2), the quantity $\hat{\sigma}$ is rewritten as

$$\hat{\sigma} = \Omega_c \left(\frac{\sigma}{\Omega_c} - \frac{mA^2}{(R/R_{\text{eq}})^2 + A^2} \right). \quad (15)$$

If this quantity $\hat{\sigma}$ becomes zero within the star, we cannot solve the eigenvalue problem because the matrix which governs the problem becomes singular as mentioned above. From Eq. (15), the quantity $\hat{\sigma}$ takes its minimum value on the rotational axis and its maximum value on the equatorial surface. Hence,

$$\Omega_c \left(\frac{\sigma}{\Omega_c} - m \right) \leq \sigma - m\Omega \leq \Omega_c \left(\frac{\sigma}{\Omega_c} - \frac{mA^2}{1 + A^2} \right). \quad (16)$$

For $m = 2$ r-modes of $N = 1$ polytropes, as seen from Fig. 1, the lower limit is always negative in the star. Thus the condition for which the quantity $\hat{\sigma}$ becomes zero can be obtained by requiring that the upper limit of $\hat{\sigma}$ must be positive inside the star. As a result, the condition that corotation points exist in the star can be written as

$$\frac{\sigma}{\Omega_c} \geq \frac{2A^2}{1 + A^2}, \quad (17)$$

where $m = 2$ is substituted because we only discuss $m = 2$ oscillation modes in this paper. In order to find out whether the corotation points appear in the star or not, we need to check this condition for oscillations of differentially rotating stars with the j-constant rotation law.

In Figure 4, values of eigenfrequencies which satisfy the *equality* of the above condition are plotted against the value of $\log A$. We will call this curve as a critical curve. If the eigenfrequency of a certain star is located above the critical curve, a corotation point appears in the star. On the other hand, if the eigenfrequency is below the critical curve, no corotation point appears. In this figure, eigenfrequencies of two equilibrium sequences, sequences with $r_p = 0.95$ and with $r_p = 0.70$, are also plotted. As seen from this figure, the eigenvalues locate well below the critical curve when the degree of differential rotation is small. When we decrease the value of A , i.e. increase the degree of differential rotation, however, the eigenfrequencies approach to the critical curve. We can infer from the result here that, for extremely slowly rotating stars for which the standard slow-rotation approximation is applied, the permitted range of the parameter A for the existence of discrete modes is *narrower* than that for rapidly rotating stars.

We show the ratio of the eigenfrequency to the critical value for appearance of corotation points in Figure 5. From this figure, it is clear that eigenfrequencies are

approaching toward the critical curve monotonically as the value of A is decreased. For nearly spherical configurations, i.e. the sequence with $r_p = 0.95$, the eigenfrequency of the model with $A = 0.615$ reaches up to 97% of the critical value. On the other hand, for rapidly rotating models ($r_p = 0.70$), eigenfrequency reaches only 93% of its critical value, when $A = 0.585$.

For slowly rotating stars ($r_p \sim 1$), sooner or later, the eigenvalues seem to cross the critical curve, though it is very difficult to get converged solutions of oscillations by using our numerical code in such cases. This is not related to the ability of the code because r-mode oscillations can be easily obtained for nearly spherical configurations with larger values of A .

For the v-constant rotation law, the condition that corotation points of $m = 2$ mode appears in the star is written as

$$\frac{\sigma}{\Omega_c} \geq \frac{2A}{\sqrt{1+A^2}}. \quad (18)$$

In Fig. 6, values of eigenfrequencies which satisfy the *equality* of the above condition are plotted against the value of $\log A$ as in Fig. 4 of the j-constant rotation law. The curves denoted by rapid rotation and slow rotation correspond to the eigenfrequencies of the equilibrium sequences with $r_p = 0.6$, and 0.95, respectively.

As seen from this figure, the eigenfrequency reaches only up to about 71 % of the critical frequency even for the model with the same axis ratio of $r_p = 0.95$, $A = 0.25$ and $T/|W| = 0.010$. It should be noted that this value of $T/|W| = 0.010$ is *smaller* than the value of $T/|W| = 0.031$ for the model with $r_p = 0.95$ and $A = 0.65$ for the j-constant rotation law. It implies that corotation points are more likely to appear for the rotation law with a steeper angular velocity distribution from the rotational axis to the equatorial surface.

4 Discussion and summary

4.1 Influence of differential rotation on the spin evolution of young hot neutron stars

It is important to know how far differential rotation will change the spin evolution scenario of young hot neutron stars by the r-mode instability. In order to get precise answer to this problem, we need to perform time evolutionary computations of rotating stars. However, it is a difficult task to do even for uniformly rotating stars. For the estimation of spin evolution of uniformly rotating neutron stars, therefore, only the growth rates of the unstable modes have been investigated by evaluating the time scales of r-mode instability due to gravitational emission and damping times of the modes due to viscosity (see e.g. [8, 9]).

Although, for uniformly rotating stars, the scheme to evaluate time scales has been already established by using the energy of the mode as measured in the rotating frame [22, 23], which is defined as a quadratic form of Eulerian perturbations, there is no corresponding definition of the energy functional which can be used to determine the stability of the oscillation modes for *differentially rotating* stars. Thus in this paper we will discuss only a tendency of evolution of differentially rotating stars via instability of the r-mode.

There are two main reasons why the r-mode instability for the uniformly rotating stars becomes important for spin evolution of young hot neutron stars. First, the growth rate of the instability due to gravitational wave emission is so large that the spin change of neutron stars would occur on a very short time scale. Second, due to the characteristic feature of r-mode oscillations, the stabilizing effect due to (bulk) viscosity is much weaker than that for the f-mode oscillations. Although it

is not easy to estimate quantitatively the effect of these two mechanisms for differentially rotating stars, we note that the time scale of gravitational emission from differentially rotating stars may be larger compared with that for corresponding uniformly rotating stars.

The energy loss rate due to gravitational wave emission can be written as

$$\frac{dE}{dt} = -\frac{1}{32\pi} \sum_{l \geq 2, l \geq m} \left(\left| {}^{(l+1)}D_{lm} \right|^2 + \left| {}^{(l+1)}J_{lm} \right|^2 \right), \quad (19)$$

where D_{lm} and J_{lm} are the mass multipole moments and the current multipole moments, respectively [24]. Here ${}^{(l+1)}D_{lm}$ and ${}^{(l+1)}J_{lm}$ are the $(\ell + 1)$ -th time derivatives of the corresponding quantities. These two multipole moments are defined as:

$$D_{lm} \equiv \int r^l \rho Y_l^{*m} d^3x, \quad (20)$$

$$J_{lm} \equiv \frac{2}{c} \frac{1}{l+1} \int r^l (\rho \vec{v}) \cdot (\vec{r} \times \nabla Y_l^{*m}) d^3x, \quad (21)$$

$$(22)$$

where c is the speed of light and Y_l^m are the spherical harmonics. Since the energy radiated away from the system is a large fraction of the rotational energy of stars (measured in the inertial frame), E_{rot} , the time scale of the gravitational wave emission, τ_{GW} , can be roughly estimated as

$$\tau_{\text{GW}} \sim \left(\frac{1}{E_{\text{rot}}} \frac{dE}{dt} \right)^{-1}. \quad (23)$$

This estimation can be applied to all rotating stars irrespective of their rotation laws.

As seen from the eigenfunctions of the perturbed velocity fields, oscillations with large amplitudes for differentially rotating stars are confined to the surface region where the density is small. On the other hand, the eigenfrequencies of differentially rotating stars are not different significantly from those of uniformly rotating stars. Thus the time derivatives of the *current multipole moments* of differentially rotating stars are considerably smaller than those of uniformly rotating stars. It implies that the time scale τ_{GW} for differentially rotating stars would be longer than that estimated for uniformly rotating stars. Therefore, the instability of r-mode oscillations of differentially rotating stars would not be so significant as that of corresponding uniformly rotating stars having the same amount of rotational energy. Of course, this must be checked by computing the growth rates of oscillations quantitatively by using such a scheme as was employed to analyze the f-mode instability of rapidly rotating stars [25].

4.2 R-mode oscillation of differentially rotating stars and the strange nature of the r-mode oscillation of the perturbational approach in general relativity

As discussed in Introduction, r-mode oscillations of neutron stars should be analyzed in the framework of general relativity. Although r-mode oscillations in general relativity have been investigated by several authors, there appear some features which do not exist in *uniformly rotating* Newtonian stars [26, 27, 28, 29, 30]. One of them is related to the strange nature of the eigenvalue problem if *barotropic* or *isentropic* configurations are treated. Some authors conclude the eigenvalue

problem becomes singular [26, 27] and other authors claim that the system results in an over-determined state [29, 30].

The strange nature of the eigenvalue problem for barotropic stars in general relativity arises from appearance of the following term in the coefficient of the highest order derivative term of the master equation if the slow rotation approximation is employed:

$$\hat{\sigma}_{\text{GR}} \equiv \sigma - m \left(\Omega - \frac{2(\Omega - \omega(r, \theta))}{\ell(\ell + 1)} \right), \quad (24)$$

where $\omega(r, \theta)$ is the dragging of the inertial frame of rotating general relativistic configurations and ℓ is the index of spherical harmonics.

If we introduce the following *effective* angular velocity

$$\Omega_{\text{eff}} \equiv \Omega - \frac{2(\Omega - \omega(r, \theta))}{\ell(\ell + 1)}, \quad (25)$$

then we can write the quantity $\hat{\sigma}_{\text{GR}}$ as follows:

$$\hat{\sigma}_{\text{GR}} = \sigma - m\Omega_{\text{eff}}. \quad (26)$$

Here, even if the stellar angular velocity, Ω , is constant value, the effective angular velocity, Ω_{eff} depends on the location. Thus the peculiar nature of the eigenvalue problem in general relativistic slow rotation approximation can be essentially the same phenomena of appearance of corotation points for differentially rotating stars which has been discussed in the previous section.

In Figure 7, distribution of the quantity $\Omega_{\text{eff}}/\Omega$ for $\ell = m = 2$ on the equatorial plane is shown for uniformly rotating general relativistic polytropes with $N = 1.0$. Relativistic polytropes are defined by the following relation:

$$p = K\varepsilon^{1+1/N}, \quad (27)$$

where ε is the energy density. The strength of gravity is measured by the ratio of the pressure to the energy density at the center [31]. Models shown in Fig. 7 are configurations with $N = 1$ and $p_c/\varepsilon_c = 0.5$ which corresponds to the typical parameter for neutron stars. Here p_c and ε_c are the central values of the pressure and the energy density, respectively. Two curves correspond to equilibrium models with $r_p = 0.97$ and 0.59 . As seen from this figure, although rotation speed of two configurations is quite different, the quantity $\Omega_{\text{eff}}/\Omega$ shows little difference. Consequently, if the eigenfrequencies of the r-mode for general relativistic configurations behave similarly as those in Newtonian models, in other words, if the eigenfrequencies tend to decrease as the stars rotate rapidly, almost the same behavior as those of differentially rotating Newtonian stars may be expected.

Therefore, there arises a possibility that the quantity $\hat{\sigma}_{\text{GR}}$ can be negative throughout the star and does not change the sign for rapidly rotating configurations as differentially rotating Newtonian stars do. In other words, the ordinary type r-mode oscillations may be possible for rapidly rotating general relativistic stars.

Moreover, as our present numerical results show, if the corotation point is about to appear in the star, it becomes very difficult to solve ordinary type r-mode oscillations, i.e. r-mode oscillations with discrete eigenfrequencies and this seems consistent with the general relativistic analysis under the slow rotation approximation. Furthermore, the eigenfunctions for such configurations behave like a delta function as seen from Fig. 2.

We may need to explain the reason why some authors [29, 30] could solve r-mode oscillations for isentropic stars in the post-Newtonian approximation. As our numerical results show, weakly or intermediately differentially rotating configurations

do not suffer from appearance of corotation points. Thus for weakly relativistic configurations, there can be the ordinary type r-mode oscillations, although they do not have exactly the same character as that of Newtonian configurations [29, 30].

From our "numerical experimental data" in this paper, there is a possibility of obtaining ordinary type r-mode oscillations for *rapidly rotating general relativistic* configurations, if one will be able to develop a scheme to handle linearized equations of the general relativistic fluid equations as well as the linearized Einstein equation for rapidly rotating stars.

4.3 Summary

We have succeeded in developing a new scheme which can be used to solve r-mode oscillations for stars which rotate differentially. This is a necessary development in order to study the scenario that neutron stars have lost their angular momentum via gravitational waves just after their birth by the r-mode instability.

By analyzing the r-mode oscillations of differentially rotating polytropes, we have shown that the eigenvalue problem is likely to become singular for configurations with large degree of differential rotation.

References

- [1] N. Andersson, *Astrophys. J.* **502**, 708 (1998).
- [2] J. L. Friedman and S. M. Morsink, *Astrophys. J.* **502**, 714 (1998).
- [3] J. L. Friedman and K. H. Lockitch, *Prog. Theor. Phys. Suppl.* **136**, 121 (1999).
- [4] N. Andersson and K. D. Kokkotas, to appear in *Internat. J. Mod. Phys. D*: preprint (gr-qc/0010102)
- [5] J. Papaloizou and J. E. Pringle, *Mon. Not. R. Astr. Soc.* **182**, 423 (1978).
- [6] J. Provost, G. Berthomieu and A. Rocca, *Astron. Astrophys.* **94**, 126 (1981).
- [7] H. Saio, *Astrophys. J.* **256**, 717 (1982).
- [8] L. Lindblom, B. J. Owen and S. M. Morsink, *Phys. Rev. Lett.* **80**, 4843 (1998).
- [9] B. J. Owen, L. Lindblom, C. Cutler, B. F. Schutz, A. Vecchio and N. Andersson, *Phys. Rev. D***58**, 084020 (1998).
- [10] N. Andersson, K. D. Kokkotas and B. F. Schutz, *Astrophys. J.* **510**, 846 (1999).
- [11] H. C. Spruit, *Astron. Astrophys.*, **341**, L1 (1999)
- [12] L. Rezzolla, F. K. Lamb and S. L. Shapiro, *Astrophys. J.* **531**, L139 (2000).
- [13] L. Rezzolla, F. K. Lamb, D. Marković and S. L. Shapiro, submitted to *Phys. Rev. D*.
- [14] L. Rezzolla, F. K. Lamb, D. Marković and S. L. Shapiro, submitted to *Phys. Rev. D*.
- [15] L. Lindblom, J. E. Tohline and M. Vallisneri, preprint (astro-ph/0010653).
- [16] S'i. Yoshida, S. Karino, S. Yoshida and Y. Eriguchi, *Mon. Not. R. Astr. Soc.* **316**, L1 (2000).

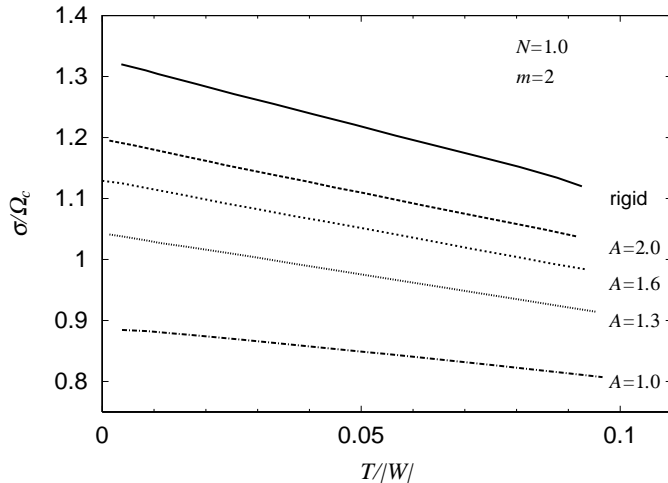


Figure 1: Eigenfrequencies for $m = 2$ mode oscillations of $N = 1$ polytropic equilibrium sequences with different values of A are plotted against the ratio of the rotational energy to the absolute value of the gravitational energy, $T/|W|$. The attached number to each curve is the value of A along the sequence. The eigenfrequency is normalized by using the central value of the angular velocity Ω_c . Terminal points of the curves for larger value of $T/|W|$ correspond to final models beyond which our numerical code could not give solutions of r-mode oscillations.

- [17] S. Karino, S'i. Yoshida, S. Yoshida and Y. Eriguchi, Phys. Rev. D **62**, 084012 (2000).
- [18] C. L. Wolff, Astrophys. J. **502**, 961 (1998).
- [19] C. L. Wolff, Astrophys. J. **531**, 591 (2000).
- [20] Y. Eriguchi and E. Müller, Astron. Astrophys. **146**, 260 (1985).
- [21] J. R. Ipser and L. Lindblom, Astrophys. J. **355**, 226 (1990).
- [22] J. L. Friedman and B. F. Schutz, Astrophys. J. **222**, 281 (1978).
- [23] J. R. Ipser and L. Lindblom, Astrophys. J. **373**, 213 (1991).
- [24] K. S. Thorne, Rev. Mod. Phys. **52**, 299 (1980).
- [25] S'i. Yoshida and Y. Eriguchi, Astrophys. J. **438**, 830 (1995).
- [26] Y. Kojima, Mon. Not. R. Astr. Soc. **293**, 49 (1998).
- [27] Y. Kojima and M. Hosonuma, Astrophys. J. **520**, 788 (1999).
- [28] H. R. Beyer and K. D. Kokkotas, Mon. Not. R. Astr. Soc. **308**, 745 (1999).
- [29] K. H. Lockitch, preprint (gr-qc/9909029).
- [30] K. H. Lockitch, N. Andersson and J. L. Friedman, Phys. Rev. D (2000) in press: preprint (gr-qc/0008019).
- [31] H. Komatsu, Y. Eriguchi and I. Hachisu, Mon. Not. R. Astr. Soc. **237**, 355 (1989).

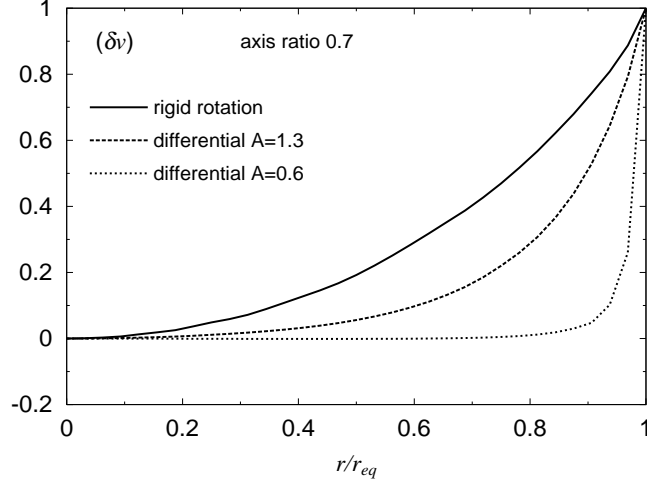


Figure 2: The θ -component of the perturbed velocity on the stellar equatorial plane is plotted against the distance from the center for $N = 1$ polytropes and the $m = 2$ mode oscillation. Three curves show distributions of the θ -component of the fluid velocity with different degree of differential rotation: the solid curve for a rigidly rotating configuration, dashed curve for a configuration with $A = 1.3$ and the dotted curve for a configuration with $A = 0.6$. The values of the axis ratio for the three models are the same, $r_p = 0.7$, and the values of $T/|W|$ are $T/|W| = 0.073, 0.082$ and 0.080 for the uniformly rotating model, the model with $A = 1.3$ and the model with $A = 0.6$, respectively. It should be noted that the large amplitude oscillations are confined to a narrow surface region for the highly differentially rotating model.

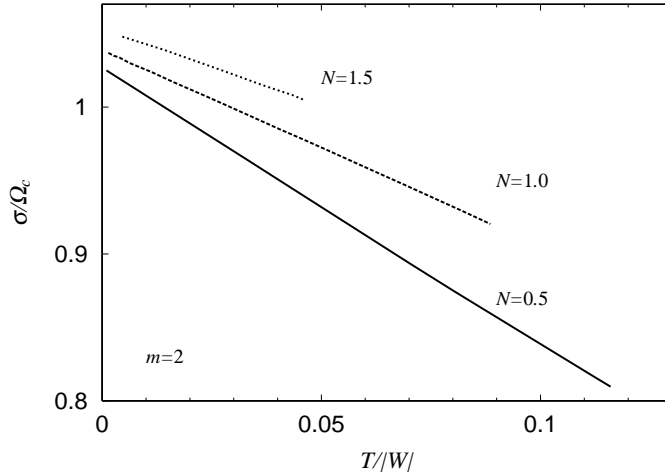


Figure 3: Same as Figure 1 but for different values of N . Attached values to the curves are the polytropic indices, $N = 0.5, 1.0$ and 1.5 . The rotation law is that of the j -constant law with $A = 1.3$.

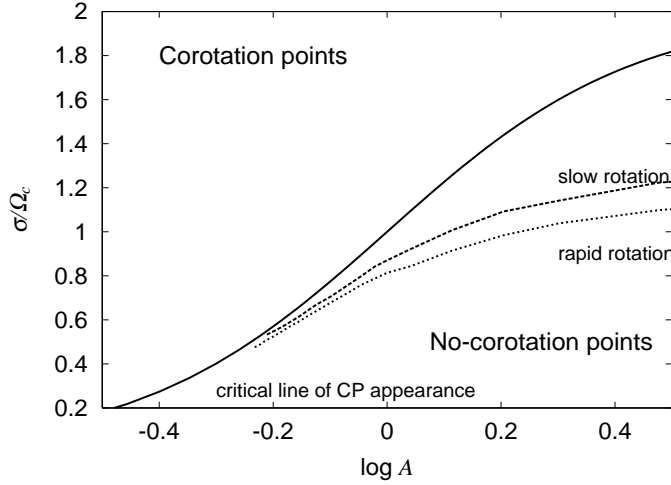


Figure 4: The critical curve for appearance of corotation points and eigenfrequencies of two equilibrium sequences are plotted against the value of $\log A$. Solid curve denotes the critical curve. Dashed and dotted curves show the eigenfrequencies for the equilibrium sequences with $r_p = 0.95$ (*slow rotation*) and 0.70 (*rapid rotation*), respectively. Terminal points of eigenvalue curves correspond to models with $A = 0.615$ for the $r_p = 0.95$ sequence, and $A = 0.585$ for the $r_p = 0.70$ sequence, respectively. The values of $T/|W|$ along the sequences are not exactly but roughly the same. For $r_p = 0.95$ sequence, $T/|W| = 0.023 \sim 0.031$ and for $r_p = 0.70$ sequence, $T/|W| = 0.078 \sim 0.080$. These terminal points of the curves for smaller values of A correspond to final models beyond which our numerical code could not give solutions of r-mode oscillations.

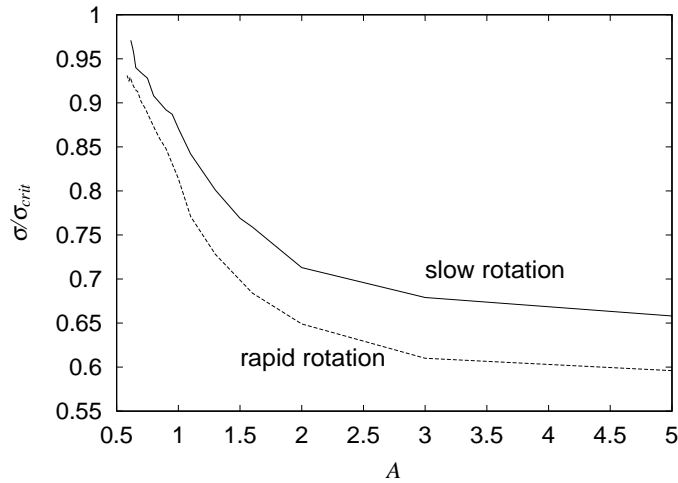


Figure 5: The ratio of the eigenfrequency to the critical value for the appearance of corotation points is plotted against the value of A . The maximum value of this ratio reaches 97% of the critical value for the appearance of corotation points along the $r_p = 0.95$ sequence.

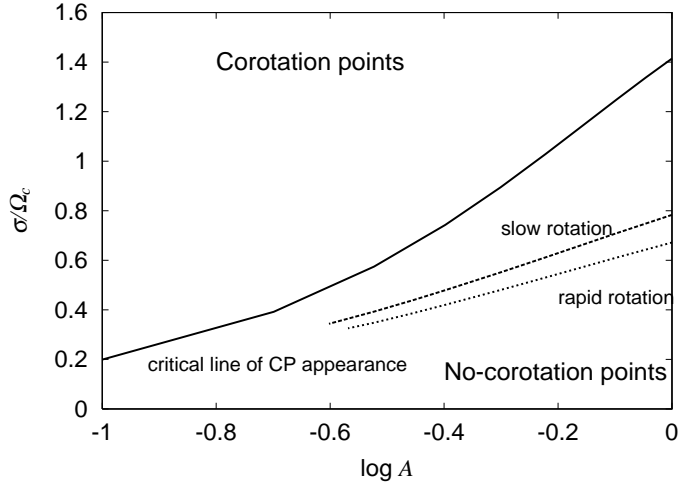


Figure 6: Same as Fig. 4 but for the v -constant rotation law. Dashed and dotted curves show the eigenfrequencies for the equilibrium sequences with $r_p = 0.95$ and 0.60 , respectively. The values of $T/|W|$ along the sequences are $T/|W| = 0.010 \sim 0.011$ for the $r_p = 0.95$ sequence and $T/|W| = 0.109 \sim 0.113$ for the $r_p = 0.60$ sequence.

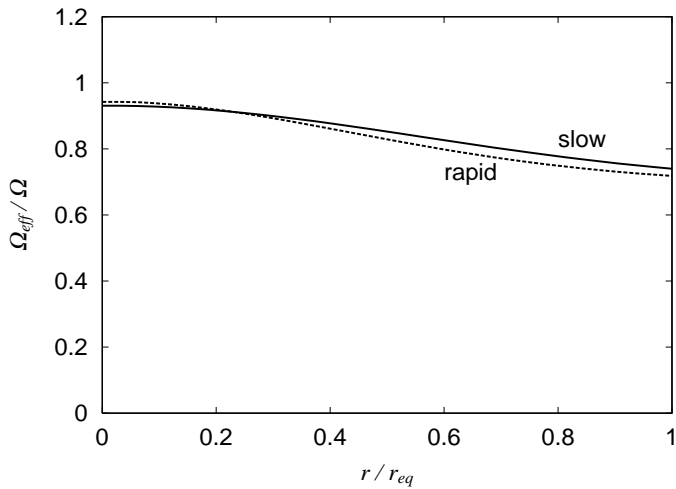


Figure 7: Distribution of the quantity $\Omega_{\text{eff}}/\Omega$ is shown on the equatorial plane of uniformly rotating general relativistic polytropes with $N = 1.0$. The strength of gravity parameter is large, i.e. $p_c/\varepsilon_c = 0.5$. The solid and dashed curves show the models with $r_p = 0.97$ (slow) and 0.59 (rapid), respectively.